Effect of HIPing on conductivity and impedance measurements of $DyBi_5Fe_2Ti_3O_{18}$ ceramics

N V PRASAD, G PRASAD, MAHENDRA KUMAR[†], S V SURYANARAYANA, T BHIMASANKARAM and G S KUMAR[*]

Department of Physics, Osmania University, Hyderabad 500 007, India
[†]Defence Metallurgical Research Laboratory, Hyderabad 500 058, India

Abstract. X-ray diffraction, a.c. impedance and conductivity (a.c. and d.c.) have been used to characterize $DyBi_5Fe_2Ti_3O_{18}$. Samples were prepared by solid state double sintering method. A few samples were also subjected to hot isostatic pressing (HIP) at 800°C for 2 h at 100 MPa pressure. The data on XRD, impedance and conductivity of two sets of samples are compared to understand study of effect of HIPing on the properties of $DyBi_5Fe_2Ti_3O_{18}$.

Keywords. Hot isostatic pressing (HIP); bismuth layered structure ferroelectrics (BLSF); ferroelectromagnetic materials; relaxor ferroelectrics.

1. Introduction

Bismuth layered structure ferroelectrics (BLSF) have received an increasing interest as high temperature piezo and pyroelectric materials since they possess high Curie temperature, anisotropic characteristics and many other interesting properties for possible device applications (Subba Rao 1962; Takenaka and Sakata 1980; Fregoso 1997). The BLSF compounds crystallize in the orthorhombic structure and are characterized by $(Bi_2O_2)^{2+}$ sheets interleaved with perovskite layers of $(A_{n-1}B_nO_{3n+1})^{2-}$ (Aurivillius 1949, 1950). For example, $Bi_4Ti_3O_{12}$ can be represented as $(Bi_2O_2)^{2+}(Bi_2Ti_3O_{10})^{2-}$ ($A = Bi^{3+}$, $B = Ti^{4+}$ and $n = 3$). In the above formula n is the number of perovskite layers in the compound. A number of compounds with the substitution of Bi^{3+} with rare earths and $B = Fe^{3+}/Ti^{4+}$ have been reported (Ismailzade 1967; Suryanarayana 1994; Singh 1996; James et al 1998; Srinivas and James 1999). In addition, the results on impedance characteristics on $LaBi_4FeTi_3O_{15}$ were also reported on the samples prepared both by uniaxial and cold isostatic pressing (James et al 1998).

In our earlier paper (Prasad et al 1998), results on $SmBi_5Fe_2Ti_3O_{18}$, which can be represented as $(SmBi_3Ti_3O_{12})$ + $2(BiFeO_3)$ or $(Bi_4Ti_3O_{12})$ + $BiFeO_3$ + $SmFeO_3$ have been reported. The present compound $DyBi_5Fe_2Ti_3O_{18}$ is analogous to the above compound. All these compounds are known to exhibit simultaneous ferroelectric and magnetic ordering. The rare earth ortho ferrite ($SmFeO_3$ or

$DyFeO_3$) have perovskite structure and belongs to a family of antiferromagnetics with unusual magnetic properties (White 1969; Gabbasova et al 1991). Gabbasova et al (1991) reported that substitution of Dy^{3+} for Bi^{3+} in small quantities showed higher magnetoelectric output. This prompted the authors to look into the effect of rare earth ions substituted for bismuth in the parent compound $Bi_6Fe_2Ti_3O_{18}$ (Prasad and Kumar 2000). While high Curie temperature in some of these compounds is an attraction for high temperature applications, there is a difficulty, since the materials do not have large remanance either in piezoelectric or piezomagnetic polarizations at a level desirable for device applications. Hence new and improved methods of processing these ceramics may result in improved material characteristics. Piezoelectric and piezomagnetic properties are essentially dependent upon electromechanical and magnetomechanical coupling respectively and these energy conversions are intimately connected with grain size and grain orientations. Hot isostatic pressing (HIP) offers the advantage of rapid densification by minimizing the time for grain growth resulting in a finer and more uniform microstructure.

The aim of the present paper is to compare the results on $DyBi_5Fe_2Ti_3O_{18}$ prepared by two processes: ceramics prepared by solid state sintering and those subjected to HIPing.

2. Experimental

The polycrystalline materials of $DyBi_5Fe_2Ti_3O_{18}$ were prepared by double sintering through solid state reaction

---

*Author for correspondence

method. Stoichiometric amounts of AR grade Bi_2O_2, Ti_2O_2, Fe_2O_3 and Dy_2O_3 were taken and thoroughly mixed and calcined at 850°C for 2 h. Pellets were obtained by uniaxially pressing the presintered powder at 8 MPa. Requisite amount of binder (polyvinyl alcohol) was added before pressing the powder. The samples were sintered at 900°C for 4 h and allowed to cool (sample A). One of the sintered pellets was subjected to hot isostatic pressing (HIP) at 100 MPa for 2 h at 800°C (sample B). The samples (A and B) were characterized by X-ray diffraction to confirm the formation of single phase. X-ray data was recorded with CuK_a radiation.

Impedance and conductivity measurements were carried out on both these samples using HP4192A impedance analyzer in a two-terminal sample holder in the frequency range 1 kHz–1 MHz and temperature region 30–500°C. D.c. conductivity measurements were made using a conventional setup. Large area faces of the samples painted with silver paint served as electrodes.

3. Results and discussion

X-ray diffractograms of both the samples (A and B) of $DyBi_5Fe_2Ti_3O_{18}$ (DBFT) are shown in figures 1a and b, respectively. The diffractograms are indexed and the lattice parameters are given in table 1. The results are compared with the $Bi_6Fe_2Ti_3O_{18}$ (BFT). The present compounds are of pseudo orthorhombic structure with slight distortion (as indicated by b/a ratio, which is very close to unity).

SEM photographs of both sintered and HIPed DBFT samples (A and B) are shown in figures 2a and b. From the photographs it is observed that, the grain sizes in samples A and B are in the range of 1–2 μm and 1–3 μm respectively. Sample B possesses plate-like structure. The clusters of small grains seen in sample A are found to disappear in sample B, where the grains are well defined and possess plate-like structure. The porosity is also found to decrease in sample B.

Figures 3a and b and 4a and b present the variation of imaginary part of impedance as a function of frequency at different temperatures for A and B samples. In sample A,

Z'' increases with the increase of frequency showing a broad peak around 500 kHz. This peak shifts to higher frequencies as the temperature is increased going beyond the range of present measurement. At all the frequencies Z'' values of sample A decrease with increasing temperature.

The Z'' values of sample B are smaller than those of sample A at all temperatures and in the frequency range studied. Sample B also shows very broad peaks in the Z'' versus frequency curves. But the peak frequencies of these samples are much lower than those observed for sample A. These peaks also shift to higher frequencies with increase of temperature.

Figure 5a shows imaginary part of impedance Z'' as a function of the real part of impedance Z' at different temperatures for sample A. These curves can be resolved into
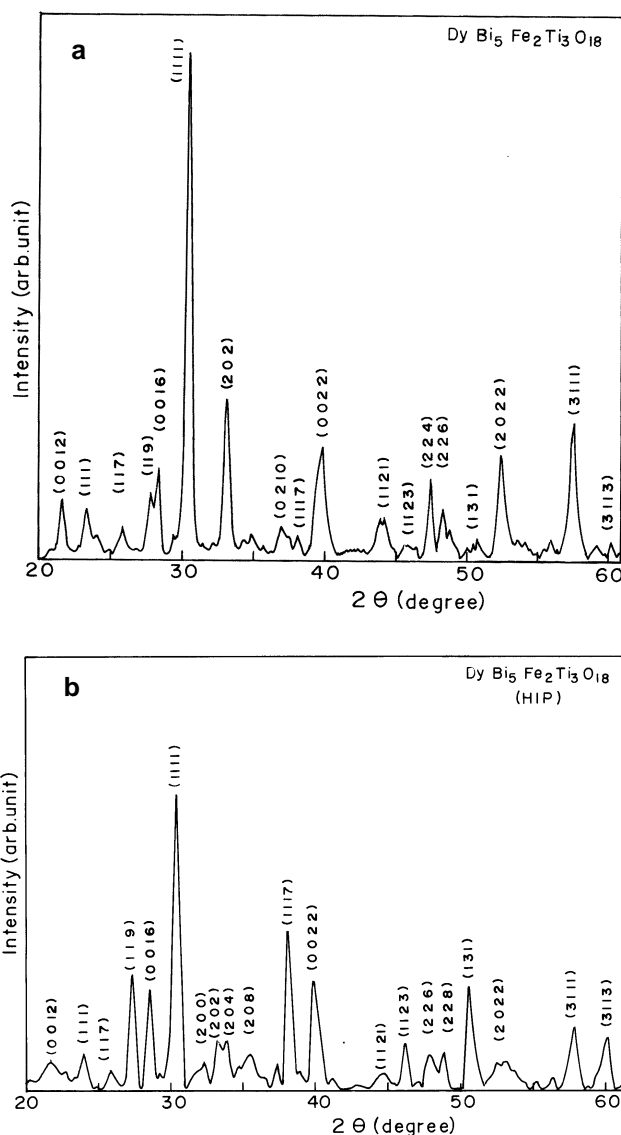
Figure 1. **a.** X-ray diffractogram of sintered DBFT (sample A) and **b.** X-ray diffractogram of sintered plus HIPed DBFT (sample B).

Table 1. Structural properties of BFT and DBFT samples.

Property	BFT	DBFT
Lattice parameter (Å)	$a = 5\cdot49$	$a = 5\cdot51$
	$b = 5\cdot50$	$b = 5\cdot48$
	$c = 50\cdot18$	$c = 49\cdot74$
Cell volume (Å³)	1515	1501
b/a ratio	1·006	0·99
Density (g/cm³)		
X-ray	7·94	7·74 (samples A & B)
Experimental	7·54	7·12 (sample A)
		7·50 (sample B)

two semicircles with their centres slightly depressed below the Z' axis. Figure 5b gives similar data for sample B.

Figures 6 and 7 present the d.c. and a.c. conductivity for samples A and B respectively as a function of inverse temperature on semilog scale.

Hot forging is known to produce grain orientation in samples (Macdonald 1987). HIP, depending on the dimensions of the samples (suitable thickness to diameter ratio) may aid grain orientation. In the present samples XRD shows decrease in the intensity of $(00l)$ reflections in sample B compared to sample A and a slight increase in intensity in the (hkl) peaks with all odd values of h, k and l. The X-ray density of sample B is 96% of theoretical density, while that of sample A is 91%. Hence in HIPed DBFT sample better densification and grain orientation is achieved. Pertinent data on structural properties of the present compound is summarized in table 1.

The impedance spectroscopy and dielectric properties of a substance form basis for most analysis of experimental data in the presence of microscopic charged inhomogeneities. Impedance is characterized by different contributions from bulk conduction, grain boundary effects and interfacial phenomenon.

Variation of Z'' with frequency at different temperatures (figures 3a and b) resemble characteristics of a relaxor ferroelectric. In the structure, the heterovalent ions (Dy^{3+} at Bi^{3+} site and Fe^{3+} in Ti^{4+} position) are randomly distributed on the cation sites in the unit cell and perovskite layers. Due to slow diffusion of ions in the thermochemical process responsible for solid state sintering of the constituent oxides, there is a possibility for micro heterogeneity in the end products. Presence of different kinds of ions in the A and B sites of ABO_3 lattice may result in localized lattice distortion.

The present compound consists of five units of ABO_3 layers. Each of these units is separated by $(Bi_2O_2)^{2+}$ layers. Because of the random occupation of equivalent sites by different heterovalent ions, there can be fluctuations in the structure giving rise to disorder, which may influence the physical behaviour under the action of temperature, pressure, electric field or magnetic field. The other aspect is the varying relaxation times. The overall effect of these results in broad peak in Z'' versus frequency plots. HIPed
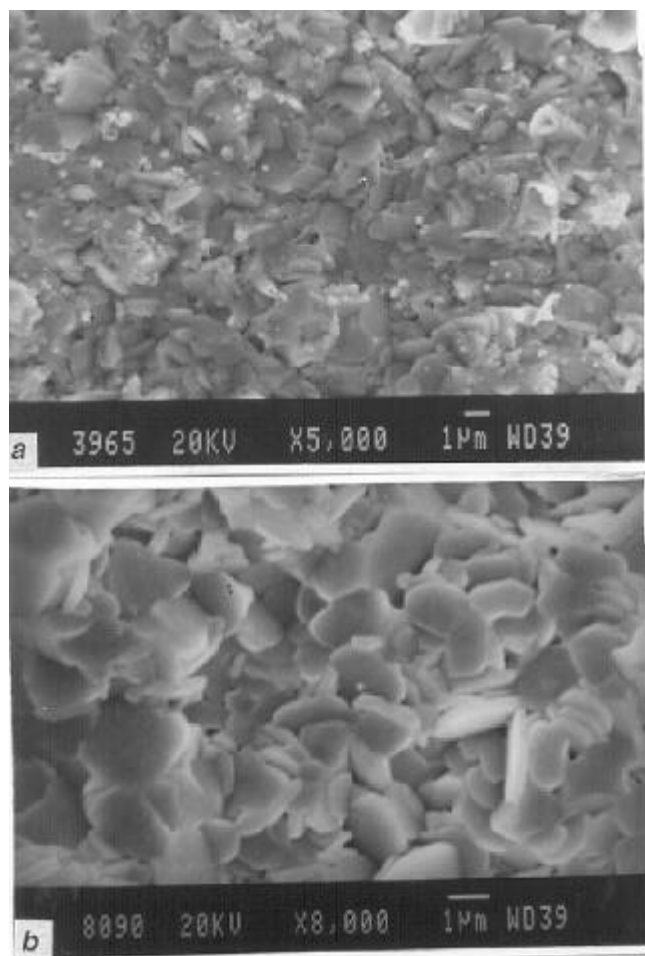
Figure 2. **a–b.** SEM photographs of sintered DBFT (sample A) and sintered plus HIPed DBFT (sample B).
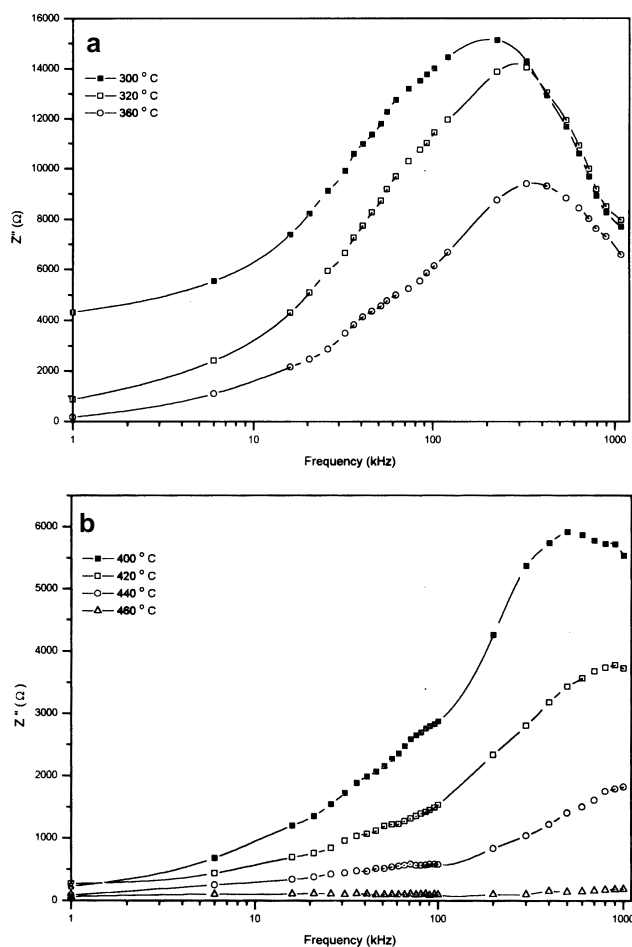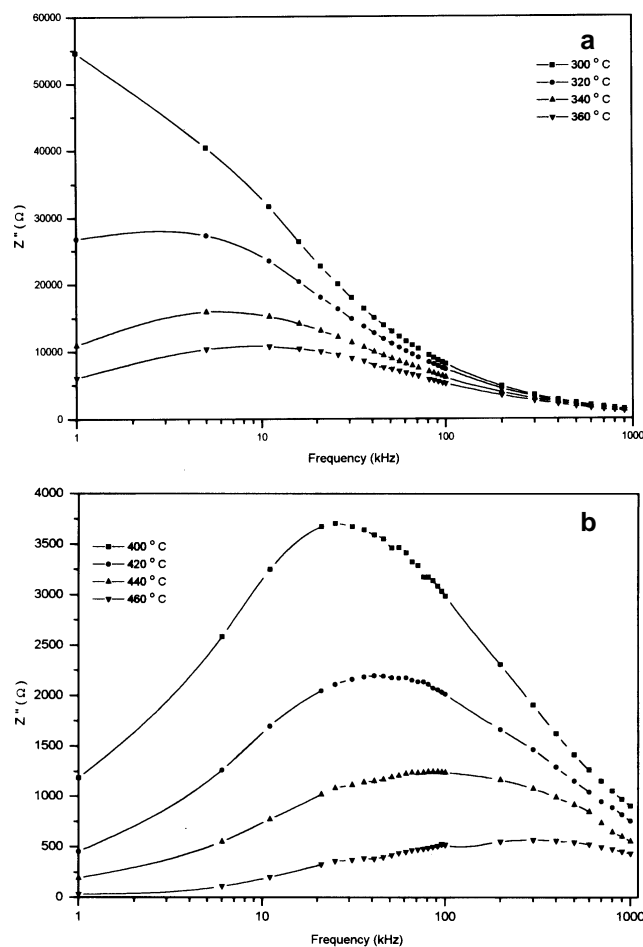

Figure 3. **a–b.** Variation of imaginary part of impedance as a function of frequency at temperature indicated for sintered DBFT.

samples have higher density and probably better grain orientation, hence HIPed have lower relaxation frequencies and larger relaxation times as observed in the present work (figures 4a and b). The relaxation times of HIPed DBFT are at least one order larger than those of sample A. The relaxation times considered here are the overall relaxation times depicting the average of all processes under way in the sample due to the application of a.c. fields.

When the continuously distributed activated energies are observed for different relaxational processes (Bunget and Popescu 1984) then,

$$t = t_0 \exp(E/kT).$$

A plot of log t vs $1000/T$ would be a straight line and the slope gives the average activation energy for relaxation of dipoles. The average values of such activation energies are found to be 0·46 eV for sample A and 0·55 eV for sample B.

The complex impedance plots (figures 5a and b) at different temperatures enable the separation of intergranular from bulk phenomenon (MacDonald 1987). At lower temperatures, the d.c. conductivity is negligible and one can observe relaxation effects in the presence of a.c. fields. The former is due to long-range effects and the latter phenomenon is due to local defect relaxation. The impedance curves beyond a certain temperature would be semicircle. Each semicircle describes relaxation of a particular class of charge entity. Since the electrode effects are small in present measurements, the two semicircles observed in the present study can be attributed to grain and grain boundary effects. Each of these contributions can be represented by parallel or series combination of RC elements. The resistance value of each element can be found from the intercept of the arc on the real axis towards low frequency side. Lower frequency arcs are due to grain boundaries and higher frequency arcs depict grain effects. Within the bulk of the material, there are two possible a.c. conduction mechanisms: first the long range a.c. conductivity and the other local transport of oxygen vacancies. The long-range conduction by vacancies and by the way of charge compensation follows the equation (Prasad *et al* 1998).

$$O_2 = 1/2\ O_2 + V_0'' + 2e^-.$$
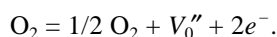
The oxygen vacancies are created due to the loss of oxygen by the material under study during sintering.

At low enough temperatures (and frequencies) the defects and charge complexes present in the sample associate giving rise to observed dielectric loss peaks due to their bound motion among all equivalent sites. The contribution to the long-range conductivity at low enough temperatures would be small and can be ignored. The long-range conductivity effects will be observable at higher temperatures. At these temperatures charge complexes may become unassociated and charges become mobile.

Grain and grain boundary resistances (r_g, r_{gb}) and relaxation times (t_g, t_{gb}, where $t = 1/w$, w is frequency at maximum arc) are functions of temperature (Bunget and Popescu 1984). When log t is plotted as a function of inverse temperature a linear plot would result. Activation energies for conduction and relaxations within the grain (E_g, e_g) and grain boundary (E_{gb}, e_{gb}) are evaluated (table 2). The activation energies for relaxation within the grain and grain boundary in sample A are smaller than those in sample B. Grain and grain boundary conduction activation energy is larger in sample A. Observed differences in the activation energies of conduction and relaxation of grain and grain boundary may be due to the grain orientation in sample B. These observations are consistent with relaxations observed in Z'' versus frequency curves.

The impedance plots of DBFT are obtained with one semicircle for temperatures below 300°C representing

Figure 4. a–b. Variation of imaginary part of impedance as a function of frequency at the temperature indicated for sintered plus HIPed DBFT.

bulk behaviour only. However, when the temperature is raised above 400°C, the semicircle representing the grain boundary effect becomes visible at lower frequencies. For HIPed DBFT, separation of grain boundary effects are visible only above 400°C. Observation of only two semi-

circles over the entire range of temperature indicates negligible interfacial and electrode processes in the present system. Figures 6 and 7 show variation of real part of a.c. conductivity of samples A and B at different frequencies. At lower temperatures there is a frequency variation of
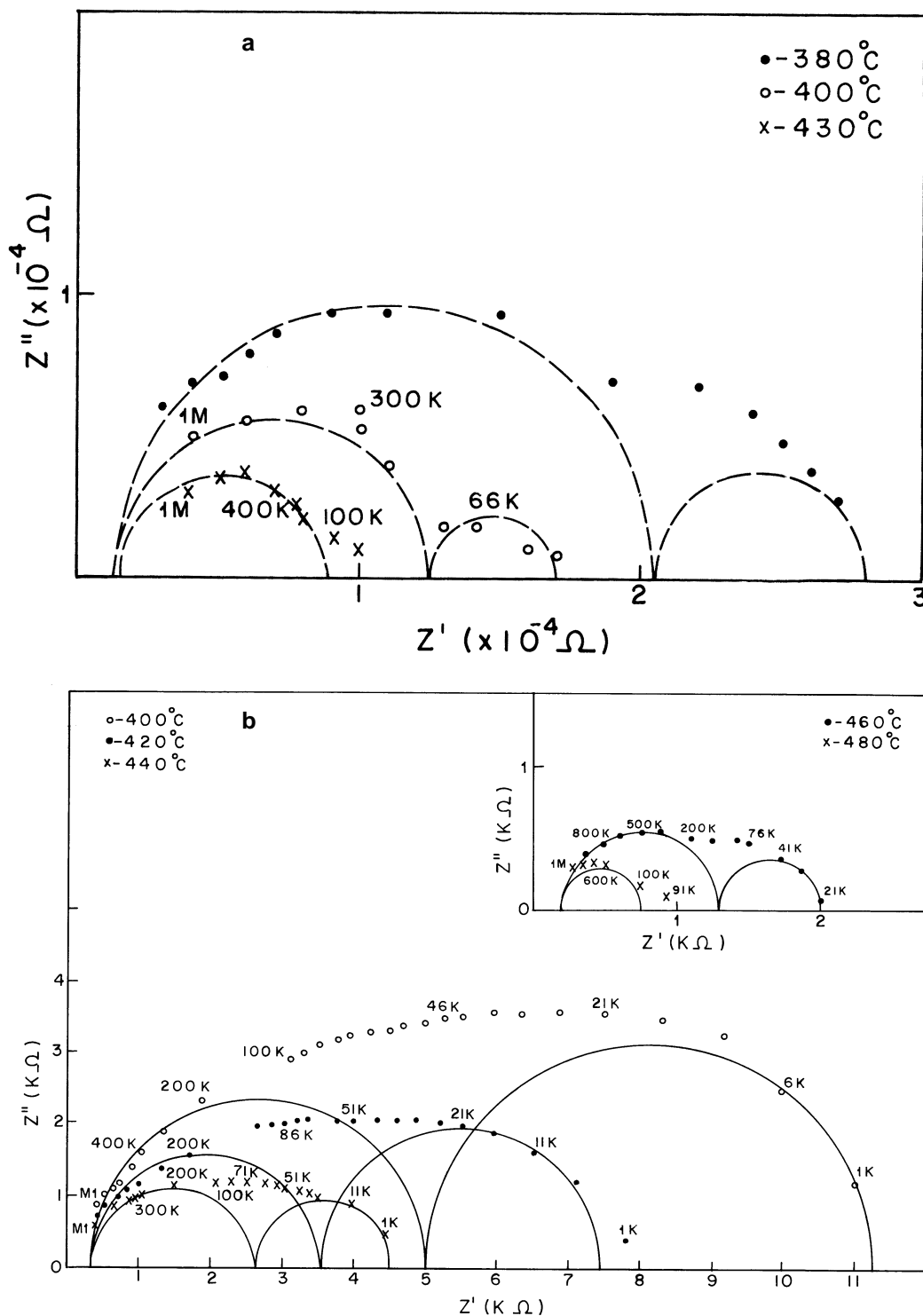
Figure 5. **a.** Variation of Z'' with Z' at different temperatures for sintered DBFT and **b.** variation of Z'' with Z' at different temperatures for sintered plus HIPed DBFT.
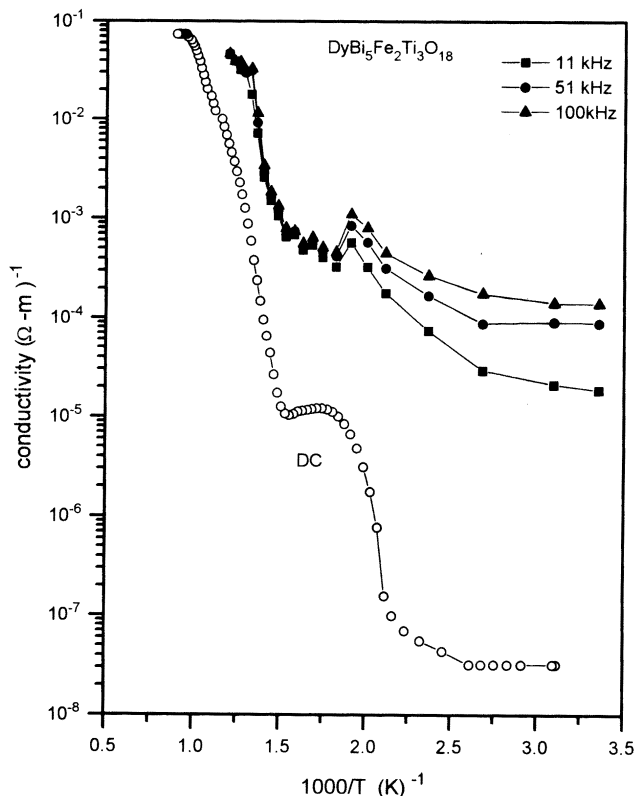
Figure 6. D.c. and a.c. conductivity as a function of inverse temperatures for sintered DBFT.
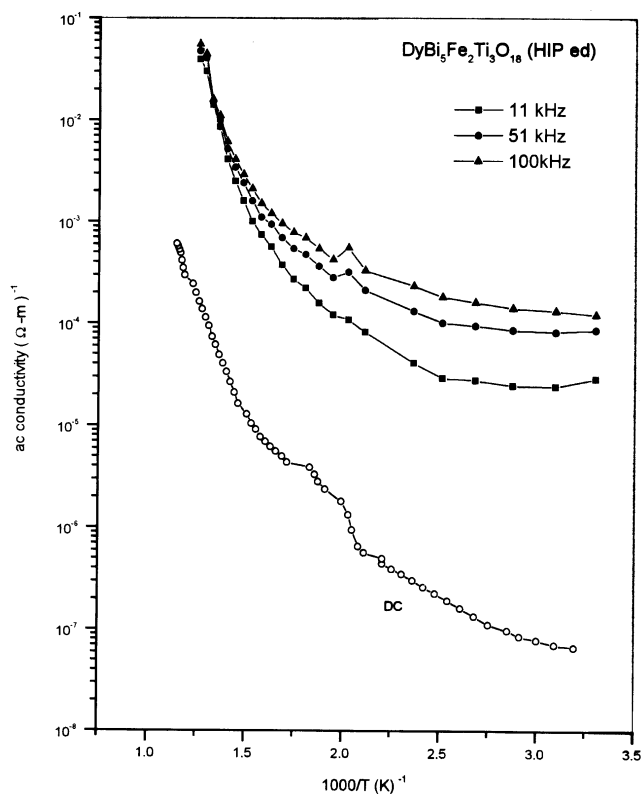

Figure 7. D.c. and a.c. conductivity as a function of inverse temperature for sintered plus HIPed DBFT.

conductivity but at higher temperatures all the conductivity curves at different frequencies merge into one indicating intrinsic conductivity. Sintered sample showed a kink around 350°C, at which a broad hump was observed in the variation of dielectric constant with temperature.

In both the samples (A and B) it is observed that the a.c. conductivity is higher than the d.c. conductivity. The admittance could not be measured at high temperatures, as the conductivity was higher than the range allowed in the impedance analyzer. The a.c. conductivity in the case of sample A shows a peak in the same temperature region at which peak was observed in the d.c. conductivity. However in sample B such peak was not observed, except at 100 kHz frequency. Activation energies have been evaluated and are tabulated in tables 3 a and b for both samples A and B. Unlike in case of d.c. conductivity, where a marked difference was observed in the variation in the two samples, the variation appears to be almost similar. This indicates that the relaxation mechanism has not been affected much because of HIPing.

It is known that the conductivity of a given sample is due to contribution from both free charge carrier motion and relaxation of dipoles. The first part of the conducti-

Table 2. Activation energies (eV) for conduction (E) and relaxation (e) for grain (g) and grain boundary (gb) in the temperature region 300–420°C.

Sample	E_g (eV)	E_{gb} (eV)	e_g (eV)	e_{gb} (eV)
Sample A	0·99	0·90	0·31	0·44
Sample B	0·73	0·87	1·23	0·61

Table 3a. Activation energies (eV) for conduction in the temperature ranges mentioned for sample A.

Temp. range (°C)	D.c. conductivity activation energy (eV)	A.c. conductivity activation energies (eV)		
		11 kHz	51 kHz	100 kHz
120–170	0·28	0·32	0·24	0·45
390–450	1·49	0·85	0·85	0·85
450–520	2·32	2·40	2·40	2·40

Table 3b. Activation energies (eV) for conduction in the temperature ranges mentioned for sample B.

Temp. range (°C)	D.c. conductivity activation energy (eV)	A.c. conductivity activation energies (eV)		
		11 kHz	51 kHz	100 kHz
120–170	0·69	0·19	0·19	0·22
320–390	0·49	0·46	0·29	0·38
390–520	0·64	1·84	1·84	1·84

vity is basically measured through d.c. conductivity, whereas the second part i.e. relaxation, is obtained from admittance of the sample measured as a function of frequency. In case of normal dielectric materials the conduction takes place through hopping between two ions of different valence states. In the present sample also there are cations with different valence states occupying both A and B sites. In addition to this, as mentioned earlier, the conduction mechanism is also through the migration of oxygen vacancies.

4. Conclusions

DyBi$_5$Fe$_2$Ti$_3$O$_{18}$ samples were prepared by solid state reaction method and also by HIPing technique (of the sintered samples) at 800°C by applying 100 MPa pressure and then show appreciable changes in relaxation time, activation energy and conductivity values. This variation is attributed to densification of the sample leading to good contact between the grains and larger grain size.

Acknowledgements

References

Aurivillius B 1949 *Arki. Kemi* **1** 463, 499
Aurivillius B 1950 *Arki. Kemi* **2** 19
Bunget I and Popescu M 1984 *Physics of solid dielectrics* (Elsevier Science)
Fregoso O A 1997 *J. Appl. Phys.* **81** 1387
Gabbasova Z V, Kuz'min M D, Zvezdin A K, Dubenko I S, Murashov V A, Rukov D N and Krynetsky I B 1991 *Phys. Lett.* **A158** 491
Ismailzade I G, Nesterenko V I, Mirishili F A and Rustamov P A 1967 *Sov. Phys. Crystallogr.* **12** 400
James A R, Kumar G S, Suryanarayana S V and Bhimasankaram T 1998 *Ferroelectrics* **216** 11
MacDonald J R 1987 *Impedance spectroscopy* (NY: Wiley)
Prasad N V and Kumar G S 2000 *J. Magn. & Magn. Mater.* **213** 349
Prasad N V, Prasad G, Bhimasankaram T, Suryanarayana S V and Kumar G S 1998 *Mod. Phys. Lett.* **B12** 371
Subba Rao E C 1962 *J. Phys. Chem. Solids* **23** 665
Srinivas K and James A R 1999 *J. Appl. Phys.* **86** 3885
Singh R S 1996 *Structure–property correlations in some magnetically ordered Aurivillius phases*, Ph.D. Thesis, Osmania University, Hyderabad
Suryanarayana S V 1994 *Bull. Mater. Sci.* **17** 259
Takenaka T and Sakata K 1980 *Jap. J. Appl. Phys.* **19** 31
White R L 1969 *J. Appl. Phys.* **40** 1061